Near-IR oxime-based solvatochromic perylene diimide probe as chemosensor for Pd species and Cu^{2+} ions in water and live cells

Poonam Sharma,[a] Sandeep Kaur,[b] Satwinderjeet Kaur,[b] and Prabhpreet Singh,[*a]

[a]Department of Chemistry, UGC Centre for Advanced Studies, Guru Nanak Dev University, Amritsar 143 005, India.

e-mail: prabhpreet.chem@gndu.ac.in; Tel: +91-84271-01534

[b]Department of Environmental and Botanical Sciences, Guru Nanak Dev University, Amritsar 143 005, India.

TABLE OF CONTENTS

1. Experimental Section

Materials and characterization*:* Chemicals and solvents were of reagent grade and used without further purification. DMSO, DMF and CH_3CN solvents were of HPLC grade. Deionized water was obtained from ULTRA UV/UF Rions Lab Water System Ultra 370 series devices. Chromatographic purification was done with silica gel 60–120 mesh. TLC was performed on aluminum sheets coated with silica gel 60 F254 (Merck, Darmstadt). NMR spectra were recorded at 400 MHz for ^1H; 100 MHz for ^{13}C (JEOL) using $CDCl_3$ as solvent. The peak values were obtained as ppm (δ) and referenced to the TMS as reference in ^1H NMR and deuterated solvent in ^{13}C NMR spectra. Chemical shift values are reported in ppm, coupling constant (*J*) in Hz and abbreviations used for splitting patterns are s = singlet, bs = broad singlet, d = doublet, dd = doublet of doublet, t = triplet, q = quartet and m = multiplet. The absorption spectra were recorded using quartz cells on Shimadzu-2450 spectrophotometer (Shimadzu, Japan) equipped with Peltier system as temperature controller and Agilent spectrophotometer. The fluorescence titrations were performed on Shimadzu RF-6000 spectroflurophotometer (Shimadzu, Japan) with excitation at 490 nm, unless otherwise stated. Theoretical calculations were carried out using DFT (B3LYP/6-31G*) basis set in the Gaussian 09 package. PDI **1** was synthesized according to previously reported literature procedure.

Method for detection of metal ions*:* Stock solutions (0.1 M) of metal ions were prepared in deionized water and were diluted as required. **OPR-PDI** was added in various 10 mL volumetric flask and subsequently different concentrations of metal ions were added. The solutions were diluted with HEPES buffer-DMSO (9:1 v/v, pH 7.2) up to the 10 mL mark.

MTT Assay: The **OPR-PDI** was used to determine the cell viability in Human Osteosarcoma MG-63 cells using MTT assay. The cells were cultured in a 96 well microplates at the concentration of 1 x 10^4 cells/0.1 ml and allow to be incubated for 24 hours for adherence. The cells were treated with different concentrations of **OPR-PDI** for another 24 hours. After incubation, thoroughly mix 20 µl of 3-(4,5-dimethylthiazol-2-yl)-2,5-diphenyltetrazolium bromide (MTT) in each well and further incubated for 4 hours to allow metabolization of MTT by the viable cells into purple colored formazan (MTT metabolic product). Finally, resuspend the intracellular MTT formazan in 100 µl of dimethyl sulfoxide. The absorbance was measured at 570 nm using a multi-well plate reader (BioTek Synergy HT).

Cell viability = Absorbance of **OPR-PDI** / Absorbance of control x 100

where

Absorbance of control = absorbance of untreated cells

Absorbance of **OPR-PDI** = absorbance of cells treated with different concentrations of **OPR-PDI**.

Cell culture: The human Osteosarcoma MG-63 cell line used in this study was obtained from National Centre for Cell Science, Pune (India). The cells were cultured in DMEM (Sigma) with 10% (v/v) Fetal Bovine Serum (Biological Industries), 100 IU/ml penicillin, 500 µg/ml of Gentamycin sulfate and 100 mg/l streptomycin (before use). Cells were grown and maintained at 37°C in a 95% humidified atmosphere, 5% CO_2 and in a fresh T-25 tissue culture flask in CO_2 incubator.
Treatment: Cells of two wells were treated with **OPR-PDI** (10 µM prepared in media with 2% DMSO); cells of 4 wells were treated with **OPR-PDI** (10 µM) for 30 minutes followed by addition of Pd^0 (2 wells each with 50 and 100 µM concentrations); cells of another 4 wells were treated with **OPR-PDI** (10 µM) for 30 minutes followed by addition of Cu^{2+} ions (2 wells each with 200 and 400 µM concentrations); 2 wells served as control.

Confocal Microscopy: MG-63 cells were seeded at the concentration of 1×10^5 cells/well in 24-well plates and 12 mm coverslip was placed in each well. The treated cells were washed two times with 1xPBS and then fixed with 4% paraformaldehyde for 10-15 minutes. After fixation, the cells were washed three times with 1xPBS. Finally, mounted the coverslips containing cells on the glass slides having anti-fading reagent (Fluoromount; Sigma). Then the image was captured at an excitation wavelength of 488 nm using Nikon A1R Laser Scanning Confocal Microscope system. The data obtained was analyzed with the software version 4.11.00 of NIS Elements AR analysis (Nikon Corporation, Japan).

Detection limit: The detection limit was calculated based on the absorbance or fluorescence titrations. To determine the S/N ratio, the emission intensity of **OPR-PDI** (10 µM) without Cu^{2+} and palladium species was measured by 3 times and the standard deviation of blank solution (without addition of analyte) measurements was determined. The detection limit was then calculated with this equation, Detection limit = 3σbi/m, where σbi is the standard deviation of blank solution (without addition of analyte) measurements; m is the slope between intensity versus analyte concentration.

Sample preparation for TLC Strips: TLC strips were made by dipping into 30% water–CH_3CN solution of **OPR-PDI** (5 µM) followed by drying under vacuum at room temperature. Different concentrations of Cu^{2+} and Pd^0 were prepared in aqueous solution. The 5 µL aliquot of each solution of Cu^{2+} and Pd^0 was added on the TLC strips previously coated with **OPR-PDI**. For control experiment, drop of water alone was also added on the TLC strip coated with **OPR-PDI**. The TLC strips were then visualized under sunlight and UV lamp on excitation at 365 nm.

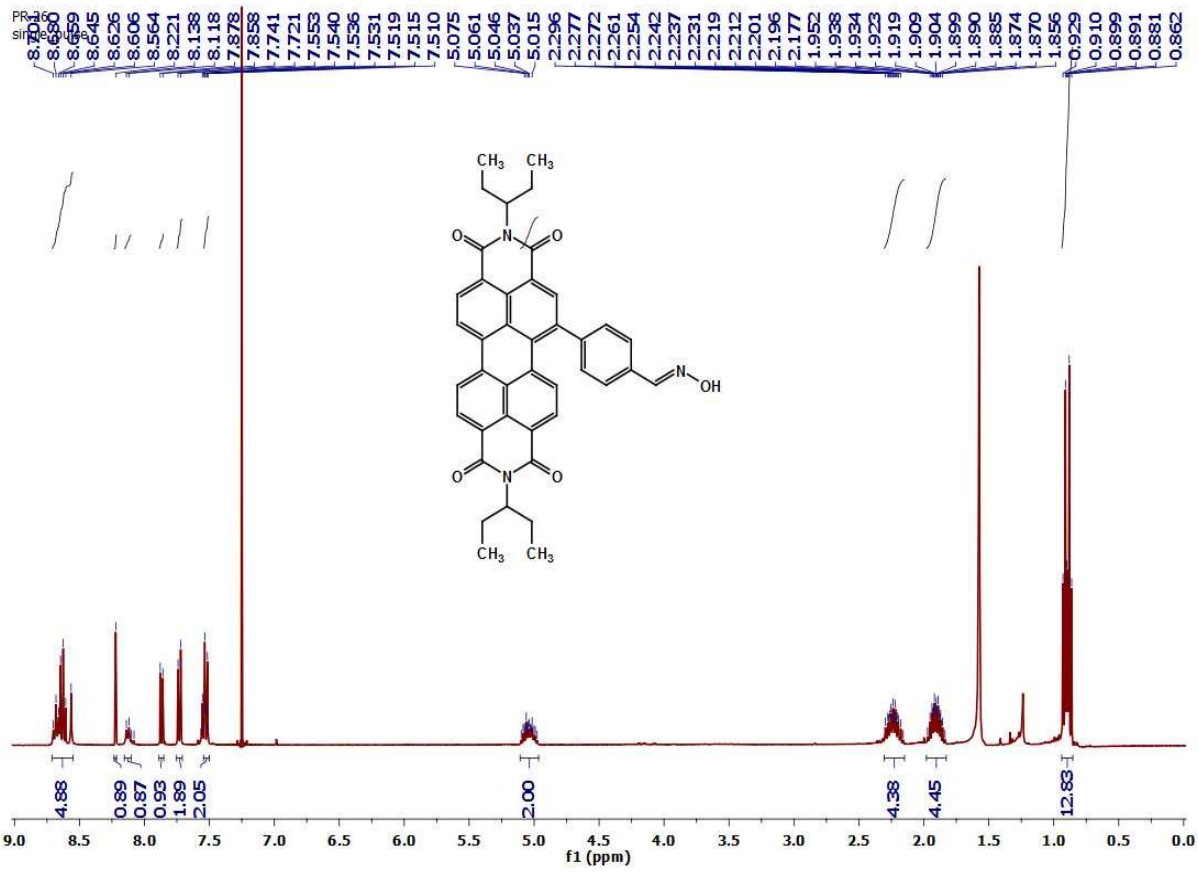

Fig. S1a: ^{1}H NMR spectrum of **OX-PDI** (400 MHz).

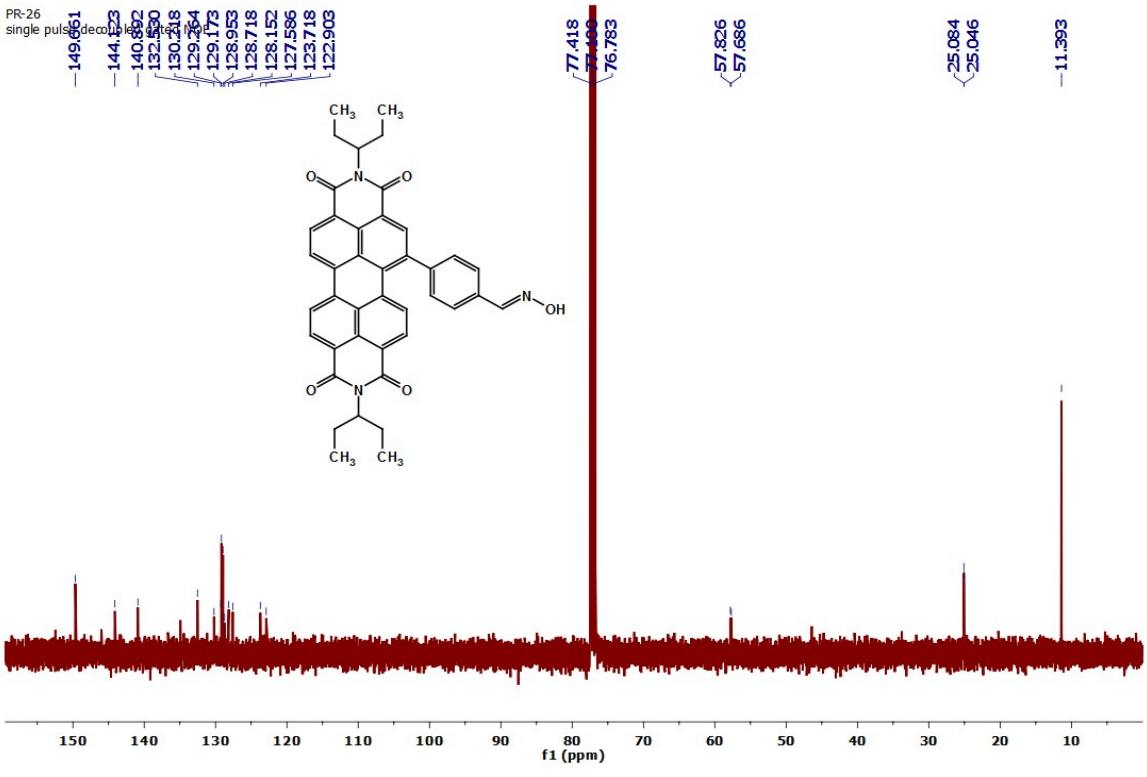

Fig. S1b: ^{13}C NMR spectrum of **OX-PDI** (400 MHz).

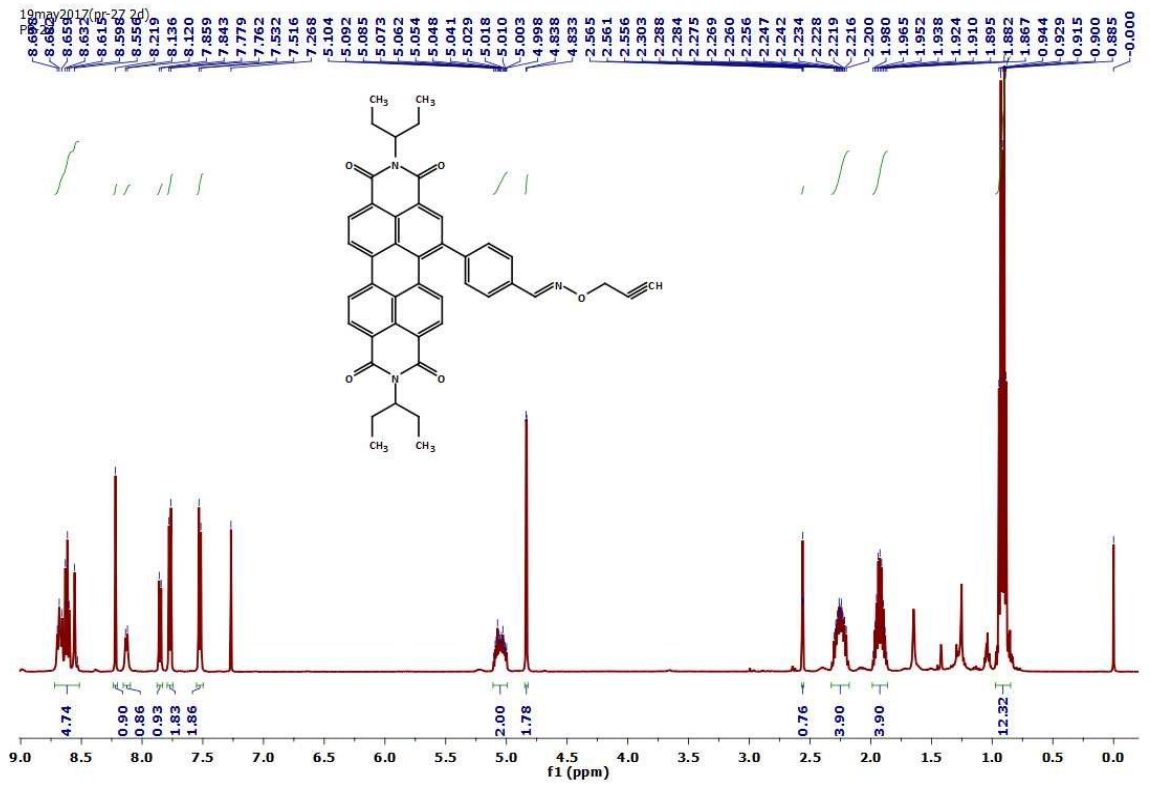

Fig. S2a: ^{1}H NMR spectrum of **OPR-PDI** (500 MHz).

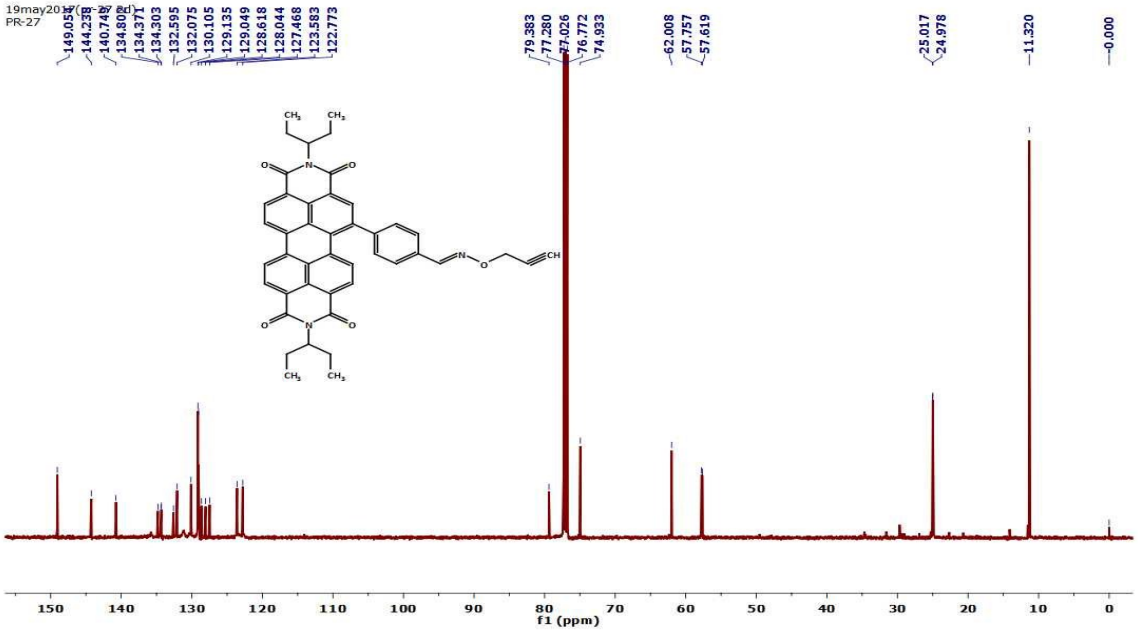

Fig. S2b: ^{13}C NMR spectrum of **OPR-PDI** (500 MHz).

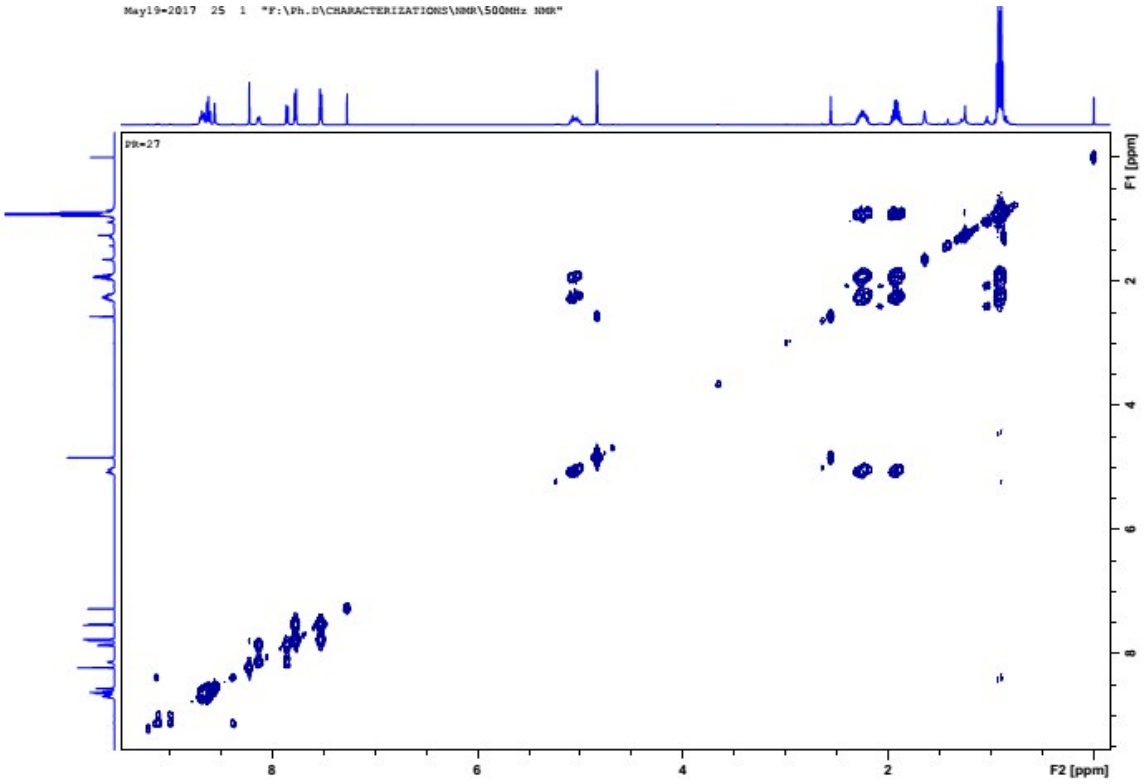

Fig. S2c: ^{1}H-^{1}H COSY spectrum of **OPR-PDI**.

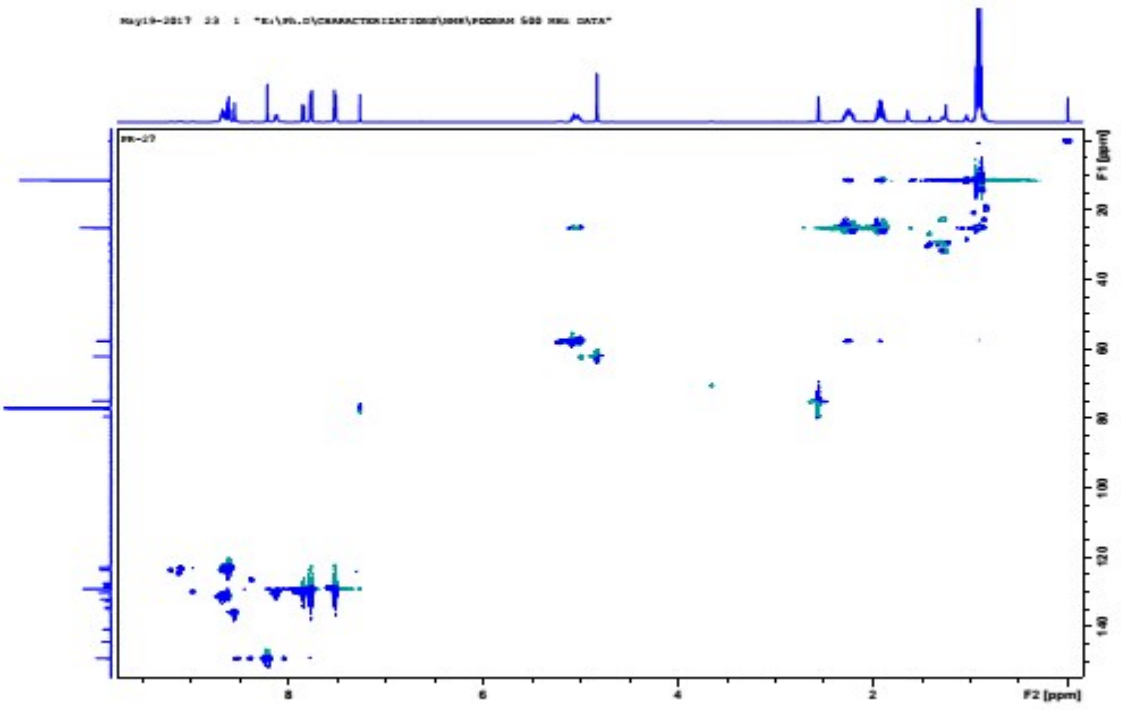

Fig. S2d: ^{1}H-^{13}C HSQC spectrum of **OPR-PDI**.

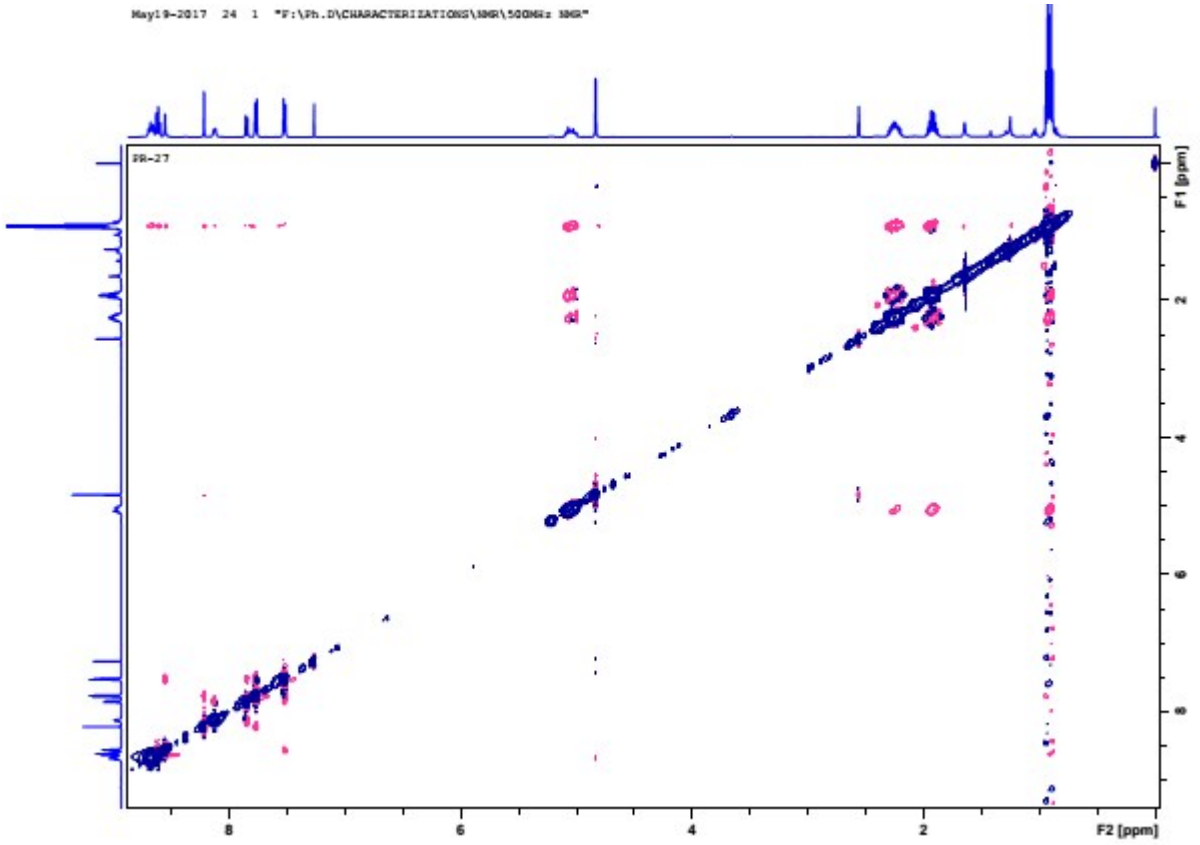

Fig. S2e: ^{1}H-^{1}H NOESY spectrum of **OPR-PDI**.

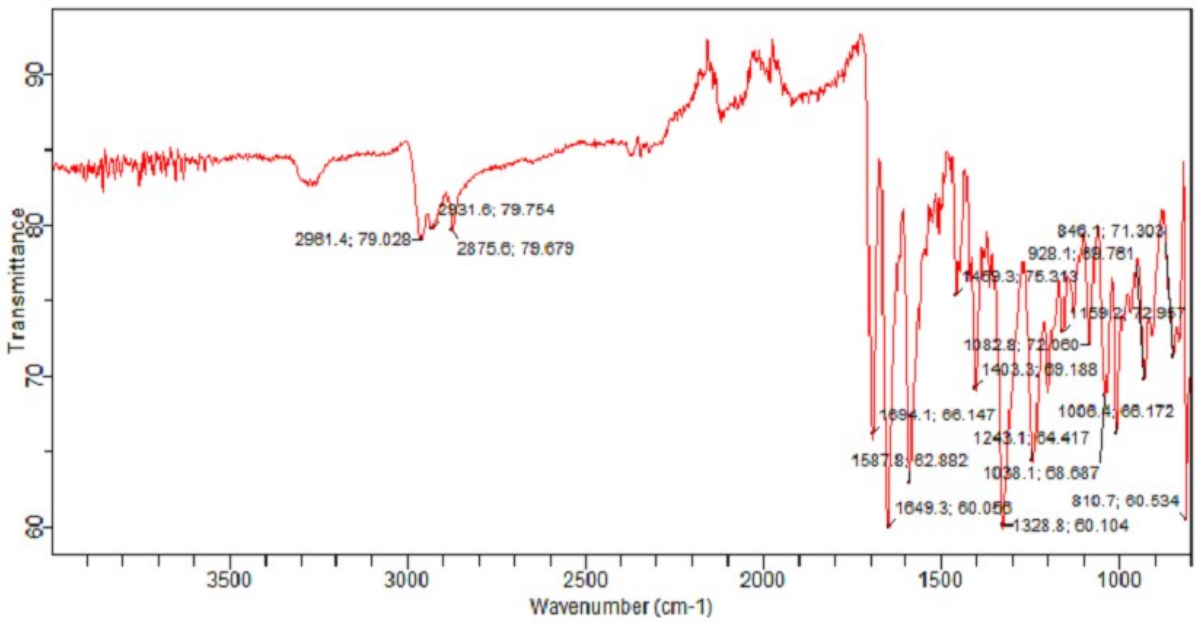

Fig. S2f: IR spectrum of **OPR-PDI**.

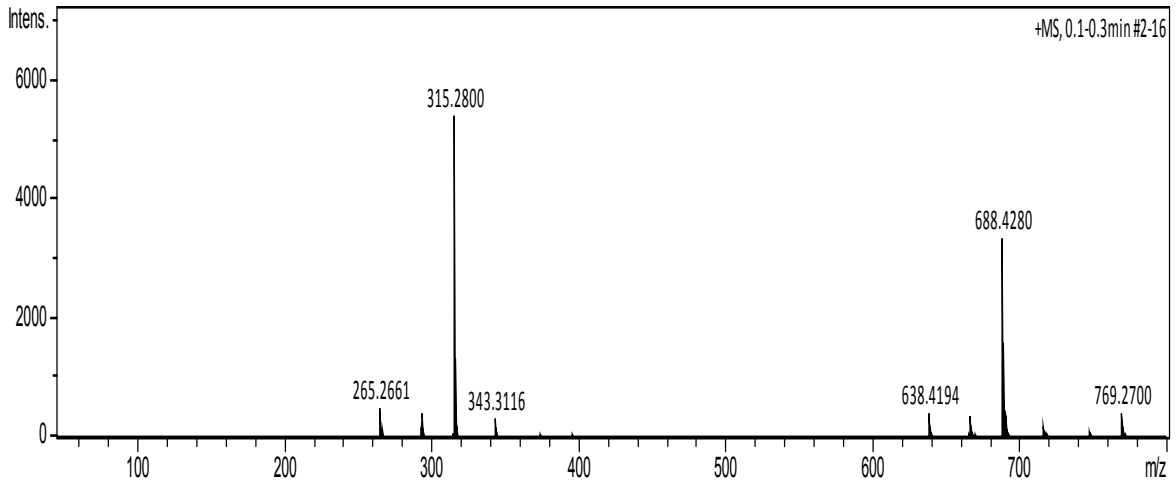

Fig. S2g: Mass spectrum of **OPR-PDI**.

2. Density Functional theory (DFT) and Time dependent (TD-DFT) calculations

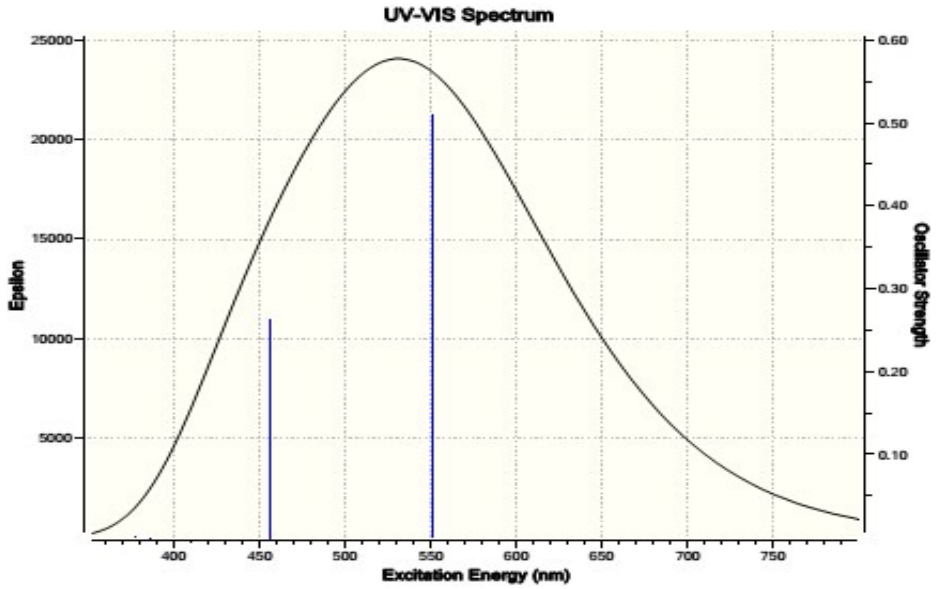

Fig. S3: Approximate excitation wavelength of **OPR-PDI** calculated by time-dependent density functional theory (TD-DFT) with the B3LYP functional and 6-31G* basis set under Gaussian 09 software. Excitation Wavelength = 550.9 nm; Oscillation Strength = 0.5111.

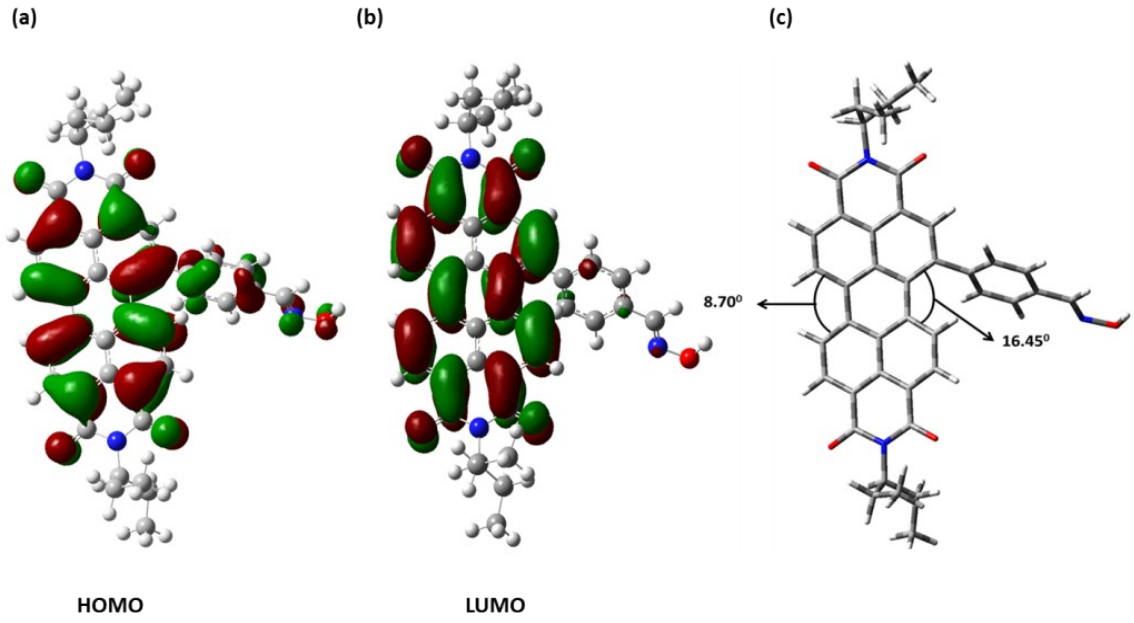

Fig. S4: (a-b) Molecular orbital analysis of PDI **2** with HOMO and LUMO presentations; (c) B3LYP/6-31G* optimized structure of PDI **2**.

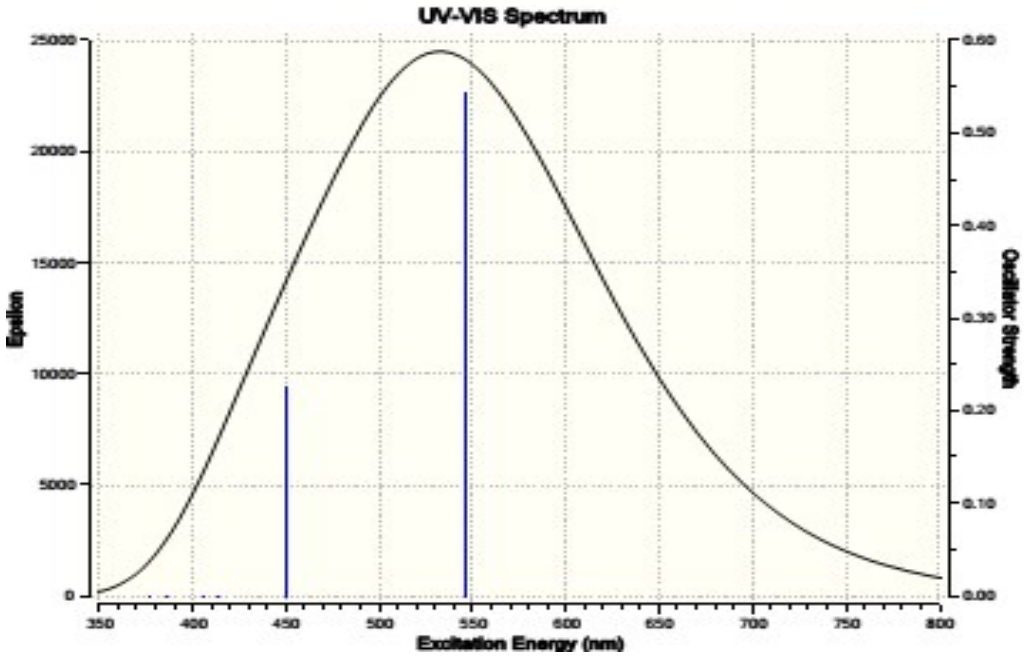

Fig. S5: Approximate excitation wavelength of PDI **2** calculated by time-dependent density functional theory (TD-DFT) with the B3LYP functional and 6-31G* basis set under Gaussian 09 software. Excitation Wavelength = 546.4 nm; Oscillation Strength = 0.5433.

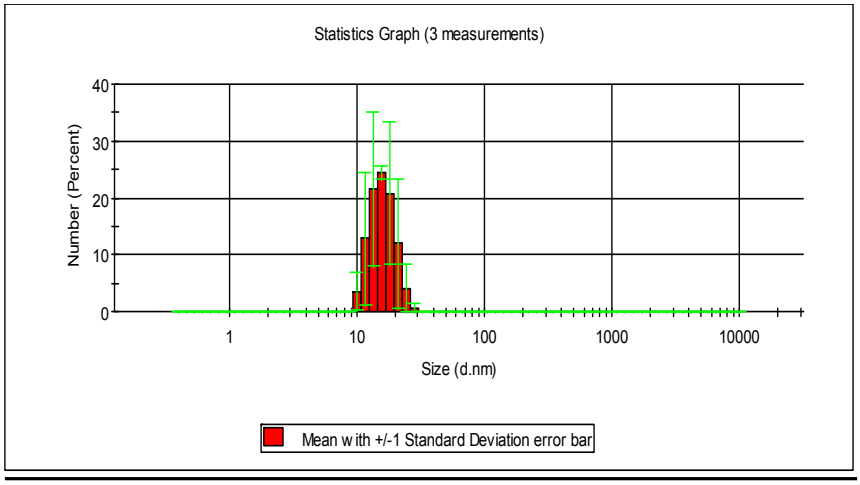

Fig. S6: DLS graph of **OPR-PDI** in CH_2Cl_2.

3. Solvatochromic properties of PDI 2

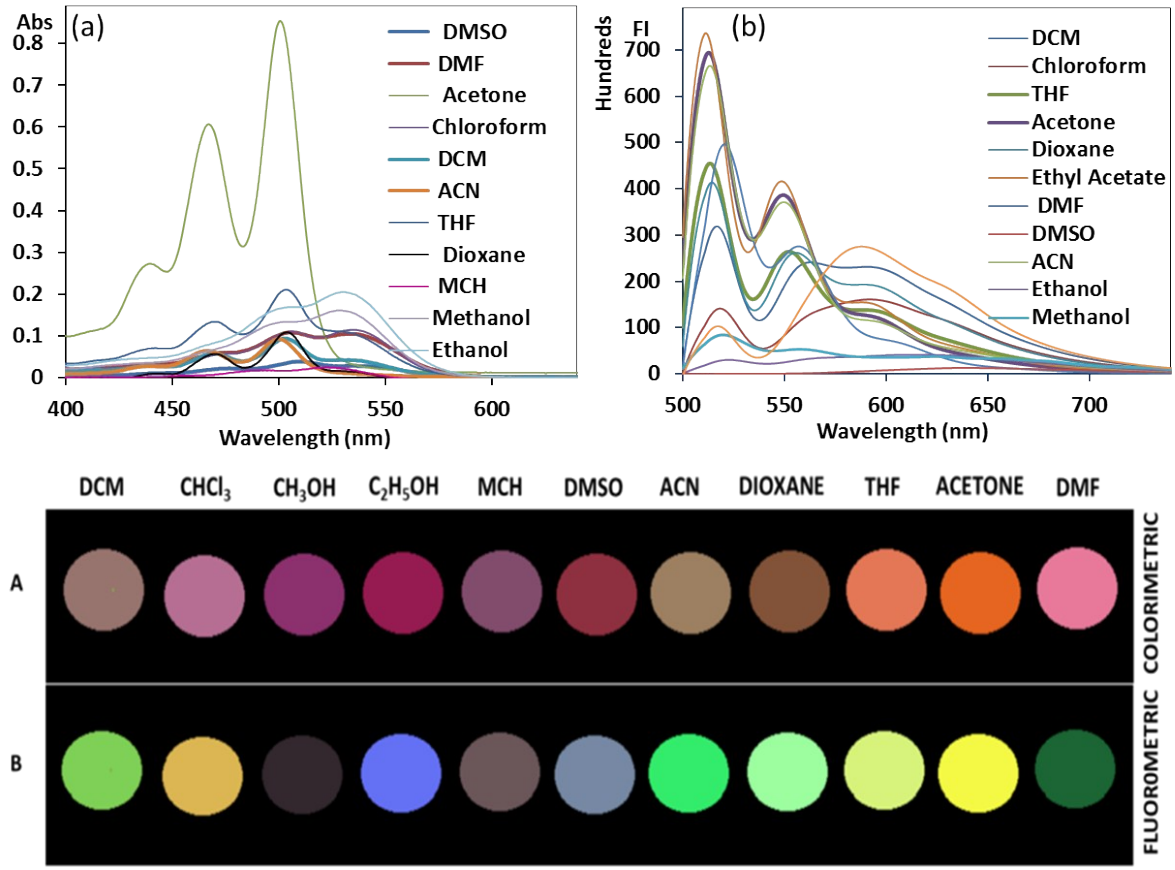

Fig. S7 (a) Absorbance and (b) emission spectra of PDI **2** (10 μM) in different polarity solvents showing solvatochromic properties; (c) photographs of PDI **2** solutions in different solvents showing absorbance and fluorescence color changes (365 nm UV lamp).

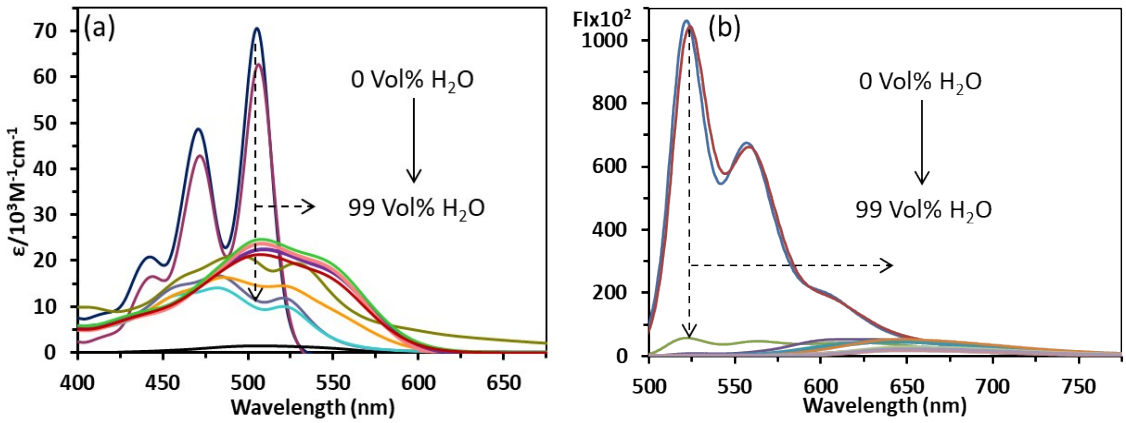

Fig. S8 UV-vis absorption and emission spectra of **OPR-PDI** (10 μM) after the incremental addition of 10 vol% H_2O in) DMF.

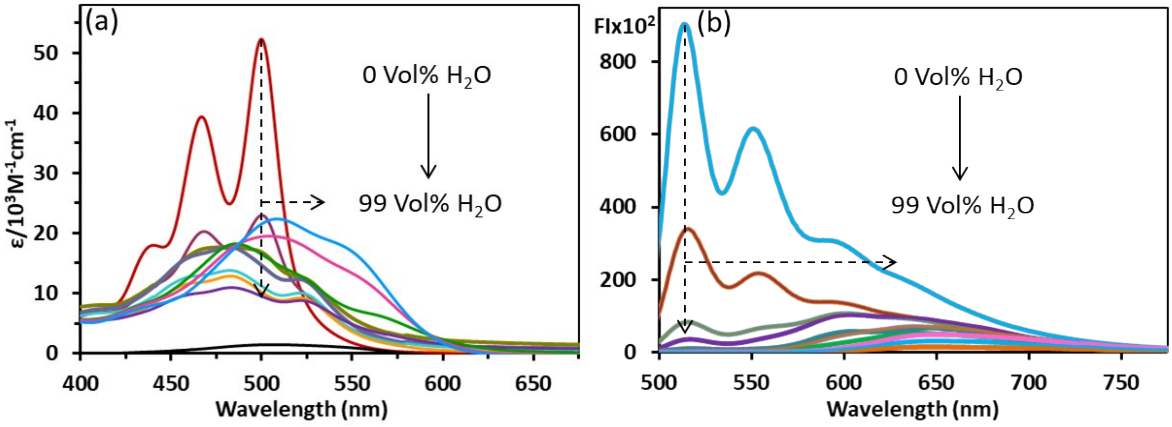

Fig. S9 UV-vis absorption and emission spectra of **OPR-PDI** (10 μM) after the incremental addition of 10 vol% H_2O in) CH3CN.

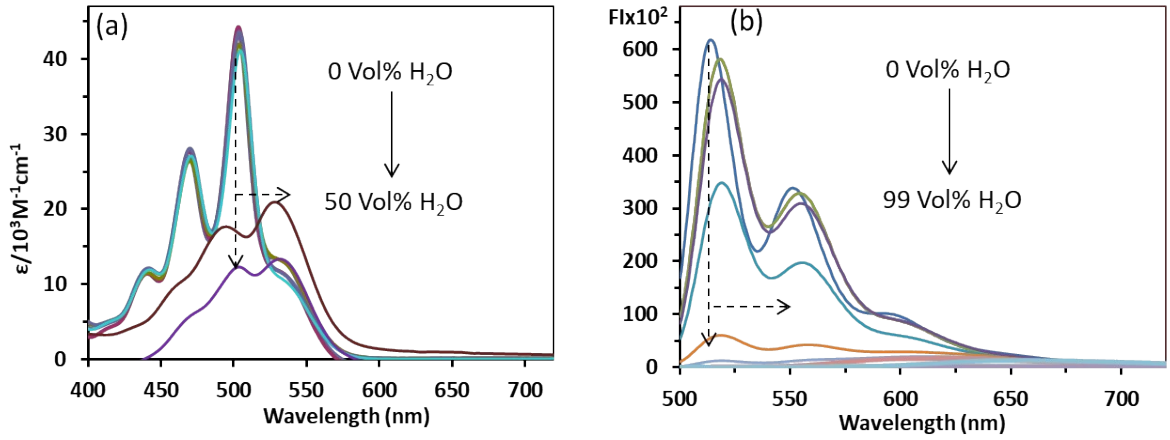

Fig. S10 UV-vis absorption and emission spectra of **OPR-PDI** (10 μM) after the incremental addition of 10 vol% H_2O in) THF.

Table S1: Frank–Codon factor (A_{0-0}/A_{0-1}) and degree of aggregation calculated for **OPR-PDI** in water-DMSO binary mixture.

Volume % Water	α_{agg}	**Frank–Codon factor (A_{0-0}/A_{0-1})**
0	0	1.46
10	0.81	1.12
20	0.95	0.72
30	0.96	0.69
40	0.99	0.71
50	0.96	0.76
60	0.95	0.76
70	0.98	0.82
80	0.99	0.90
90	1	1

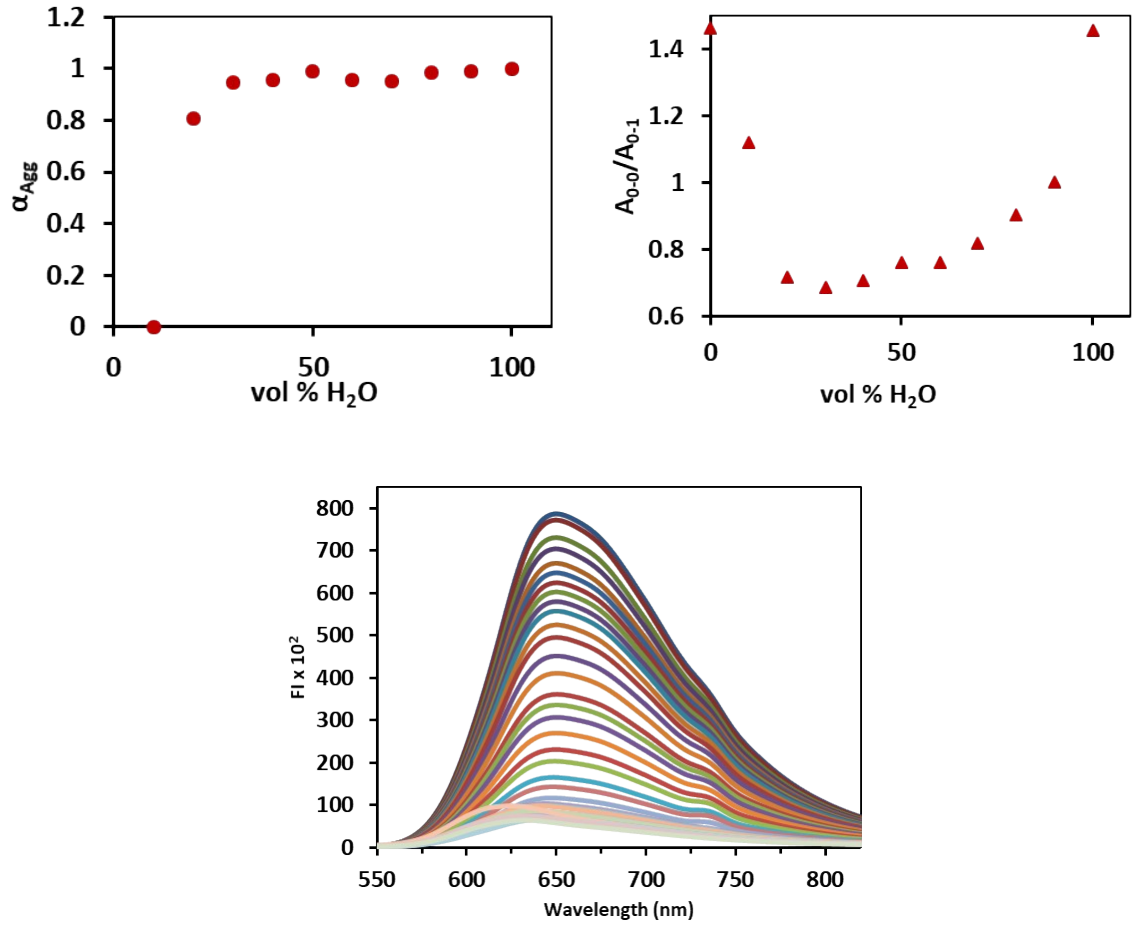

Fig. S11: Emission spectrum for Pd^0 showing blue shift.

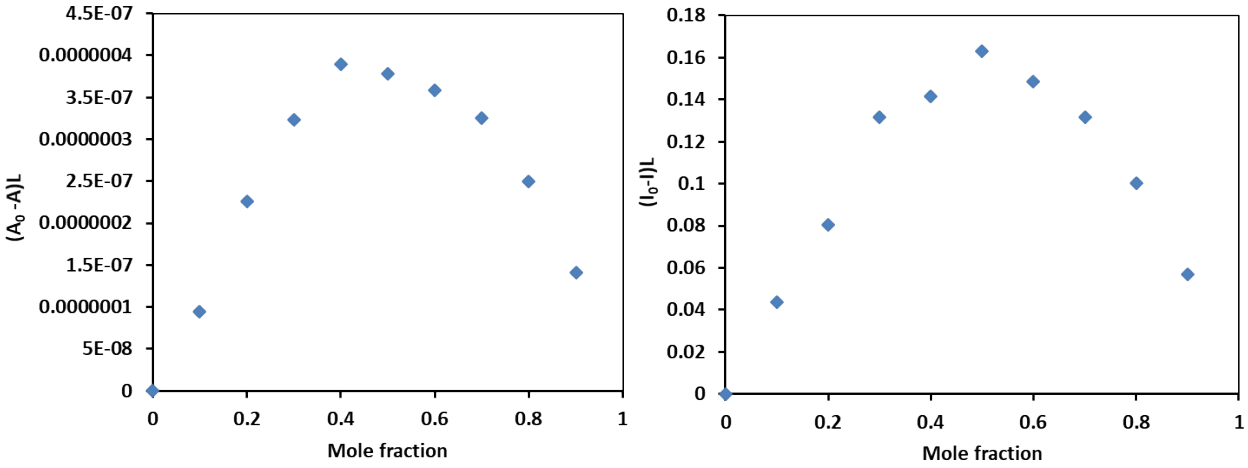

Fig. S12: Jobs plot based on colorimetric and fluorometric data.

Table S2: Recovery in percent of Pd^0 and Cu^{2+} ions in biofluid samples using fluorometric technique.

		Pd^0			**Cu^{2+}**		
Techniques	**Samples**	**Pd^0 added (µM)**	**Pd^0 found (µM)**	**% age recovery**	**Cu^{2+} added (µM)**	**Cu^{2+} found (µM)**	**% age recovery**
Fluorescence	**Blood Serum**						
		5.75	5.9	102.6	**ND**	**ND**	**ND**
		7.25	7.0	96.5	**ND**	**ND**	**ND**
	Urine	0.4	0.39	98.7	0.3	0.32	106.6
		2.25	2.15	95.5	1	1.05	105
		3.25	3.15	96.9	9	9.25	102.8
		3.75	3.95	105.3	28.3	27.8	98.2

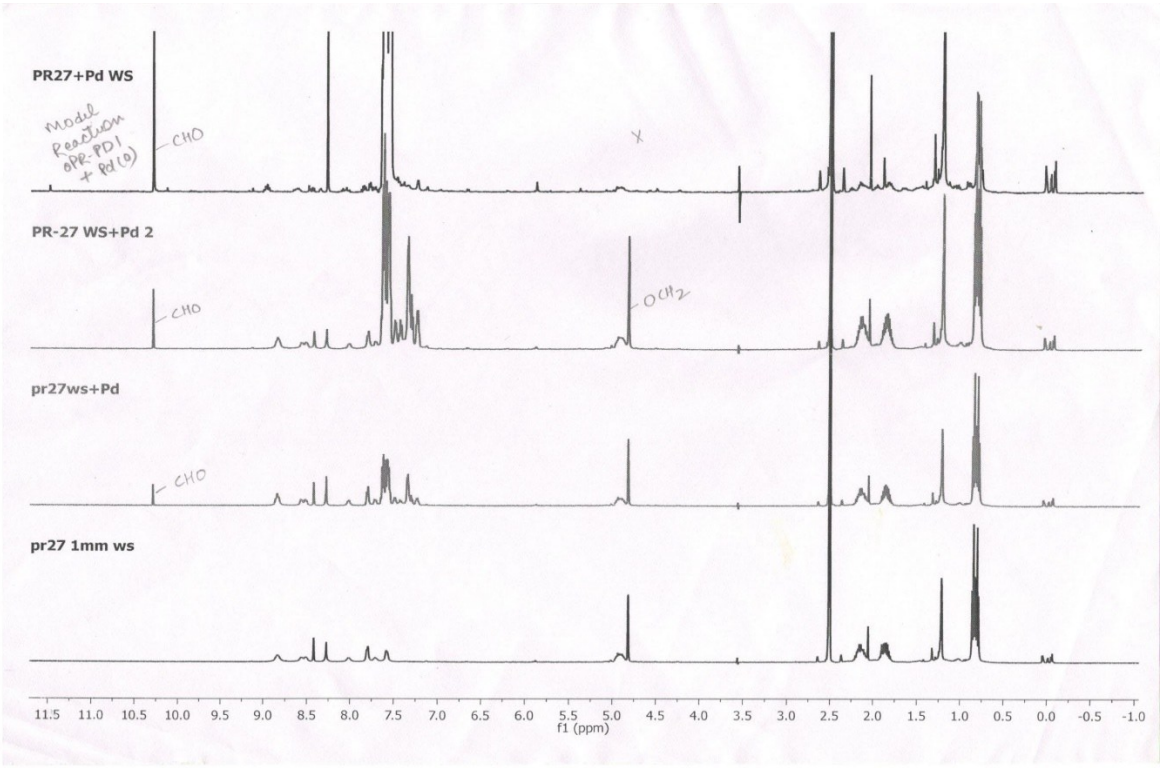

Fig. S13: ^{1}H NMR spectra of **OPR-PDI** recorded in DMSO (d_6) on incremental addition of Pd^0 (1 and 2 equivalents) and for comparison ^{1}H NMR spectra of product obtained from model reaction at the top has been given.

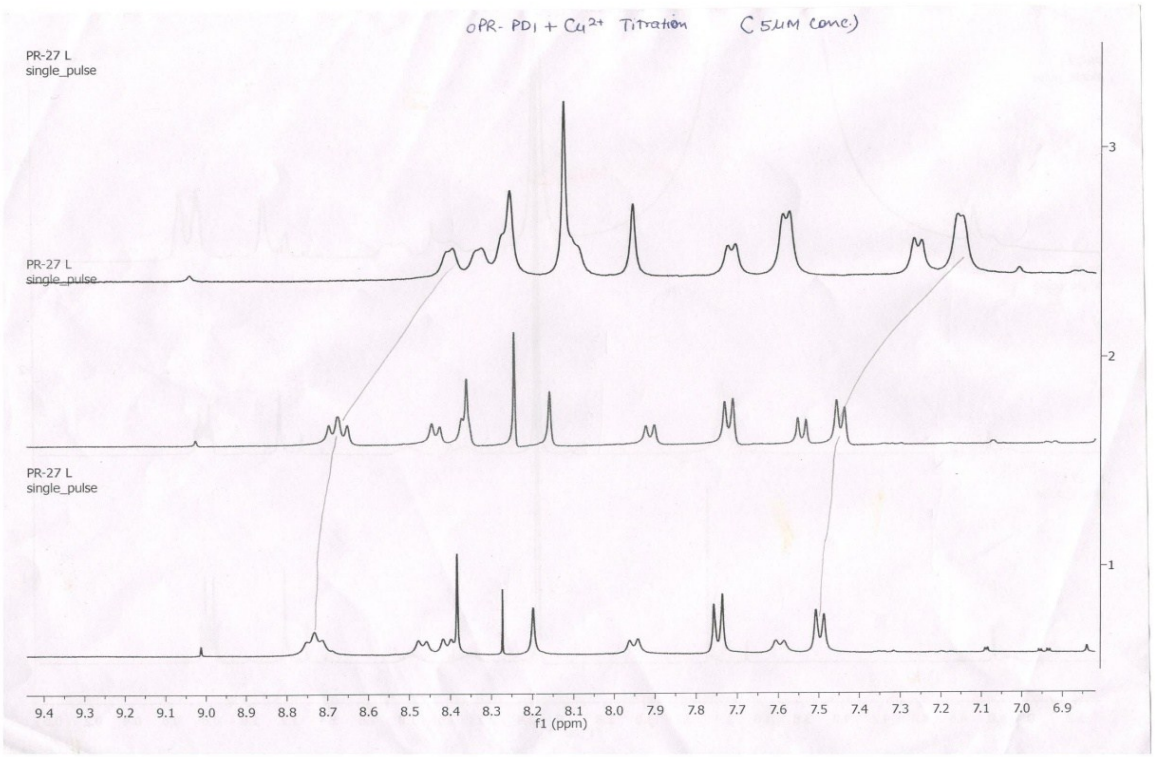

Fig. S14: ^{1}H NMR spectra of **OPR-PDI** recorded in DMSO (d_6) on incremental addition of Cu^{2+} ions (1 and 2 equivalents).